SECTION 4

EXPERIMENTAL RESULTS

4.1 System Identification

4.1.1 Response of Pressure to Control Signal

The response characteristics of pressure to control signal have been identified by the shaking table experiment performed under El Centro 300 gal excitation in Series 2 (bang-bang control). The control signal was switched between 10 kgf/cm^2 and 45 kgf/cm^2. One set of the recorded time histories observed in this experiment are shown in Fig. 4.1.

A first order time delay model is assumed between the control signal and the pressure response as described in Eq. 2.6. The time constant T in the equation has been identified by minimizing the sum of the square errors between the pressure response from the experiment and that from the computer simulation. It is observed that the time delay of the pressure response to the control signal depends on whether the pressure is increased or decreased. Therefore, the time constants T_i under increasing pressure and T_d under decreasing pressure are identified separately as shown in Figs. 4.2 and 4.3. Figure 4.2 plots the sum of the square

error defined as $\sum_k (p_{sim}(t_k; T_i) - p_{exp}(t_k))^2$ where $p_{exp}(t_k)$ = pressure value observed in the experiment at $t = t_k$, and $p_{sim}(t_k; T_i)$ = simulated value at $t = t_k$ with T_i being used as time constant. The summation is over those time intervels in the entire time history where the pressure increases. Figure 4.3 plots the sum of the square errors for the time intervals where pressure decrease. The curves in these two figures indicate reasonably well defined optimal values for T_i and T_d, with $T_i = 0.029$ sec and $T_d = 0.035$ sec.

Figure 4.4 shows, in solid line, part of the time history of pressure response from the bang-bang control experiment. Also the pressure response obtained by computer simulation is shown in Fig. 4.4, in dashed line, using the first order time delay model of Eq. 2.6 with the optimal values of the time constants identified above. The simulation result is in good agreement with the experimental result, implying that the analytical model for the relationship between pressure response and control signal, Eq. 2.6, with the identified value of time constants represents the reality very well.

4.1.2 Relationship Between Friction and Pressure

In the structural model considered, the absolute value of response acceleration equals the normalized friction force f ($f = \mu\ g$) when the model is sliding as indicated in Eq. 2.2. Therefore, the response acceleration detected from the sensor can be used to study the behavior of the friction. From the response acceleration observed in Experimental Series 1 (passive isolation) conducted at various levels of constant pressure under El Centro excitation, the relationship between pressure p and normalized friction force f is identified.

As shown in Fig. 4.5, the relationship between the pressure and the normalized friction force follows a linear relationship. The coefficient of friction μ of about 10.2% at the pressure

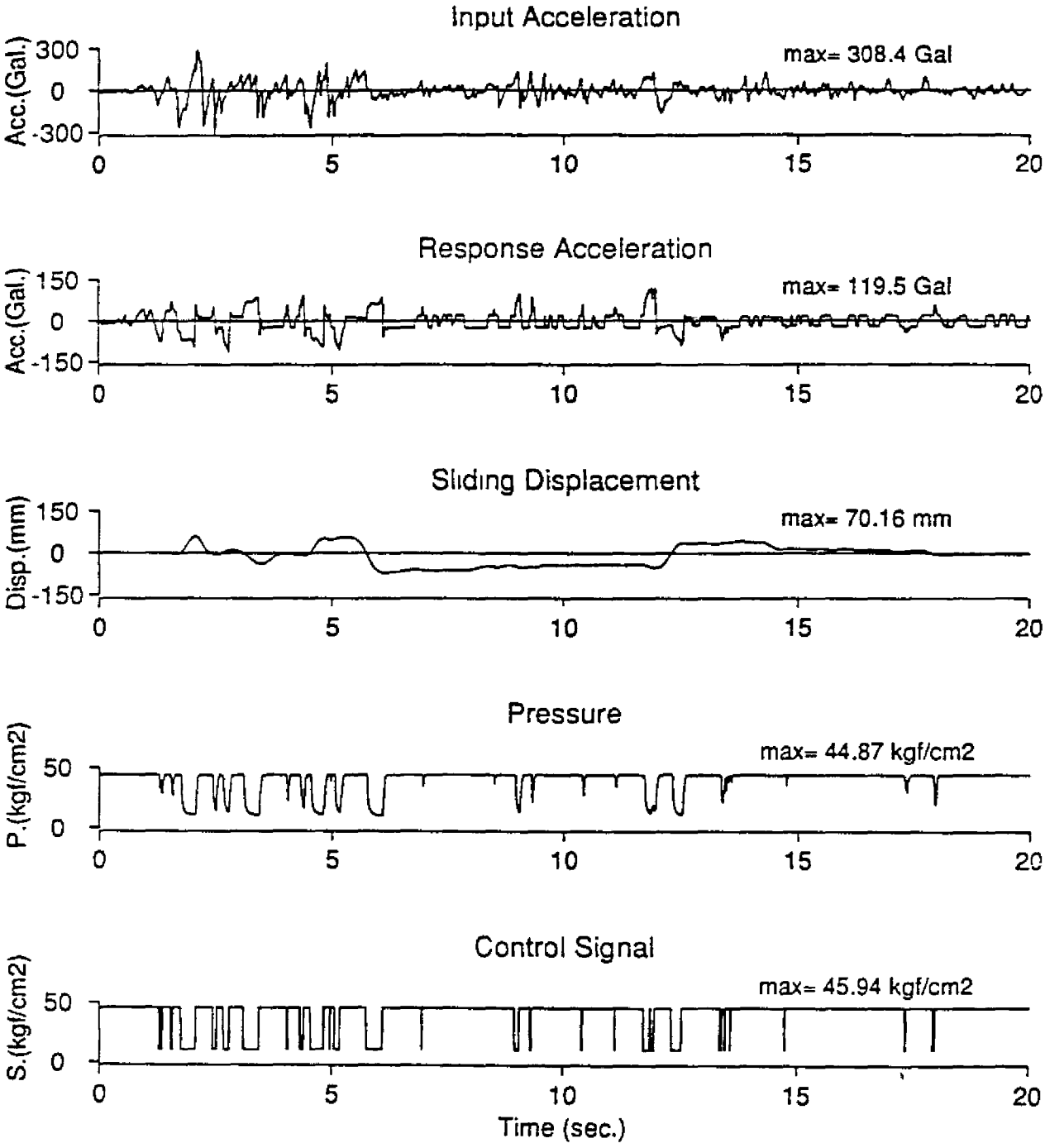

Figure 4.1: Bang-bang Control (Experiment)

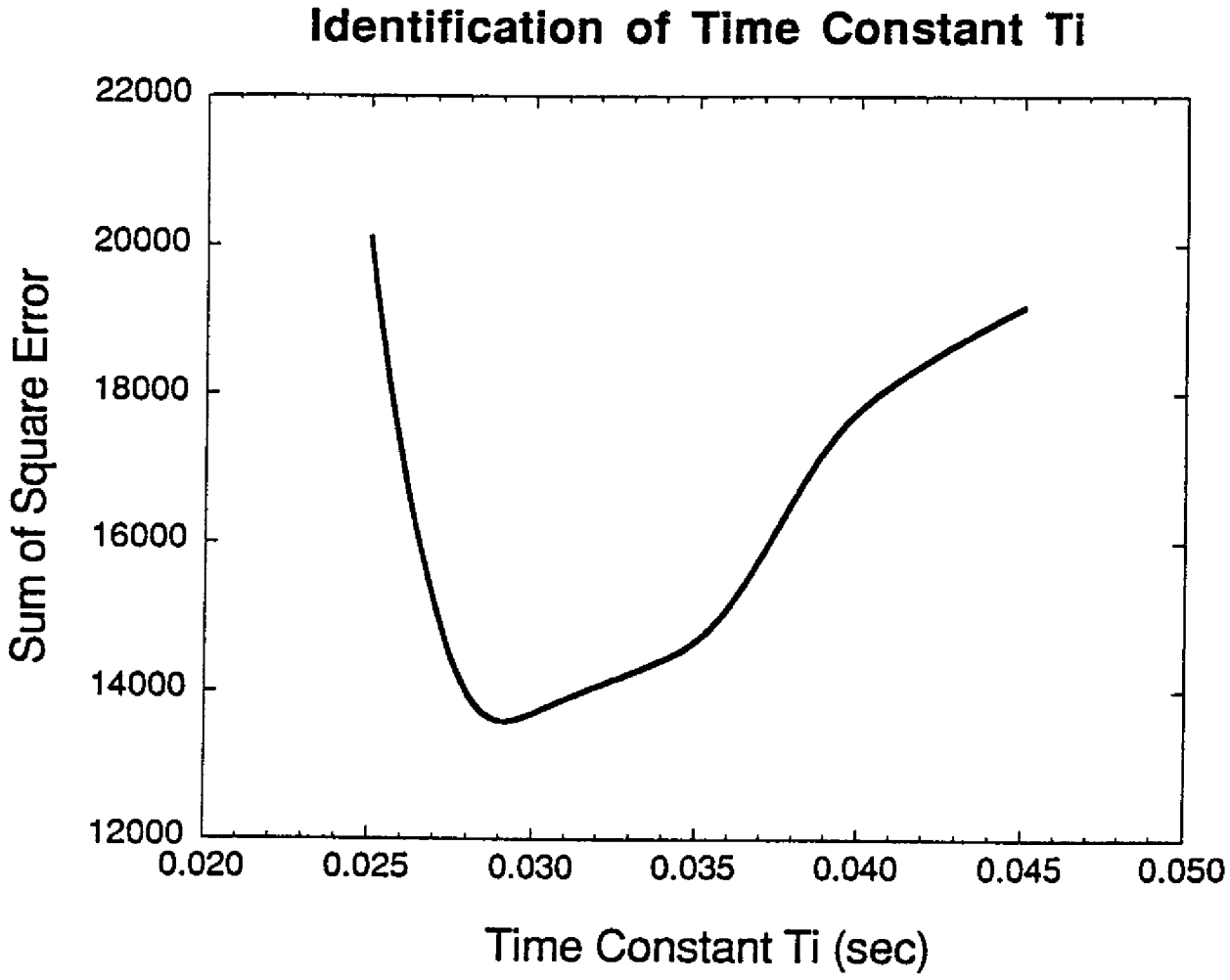

Figure 4.2: Identification of Time Constant T_i

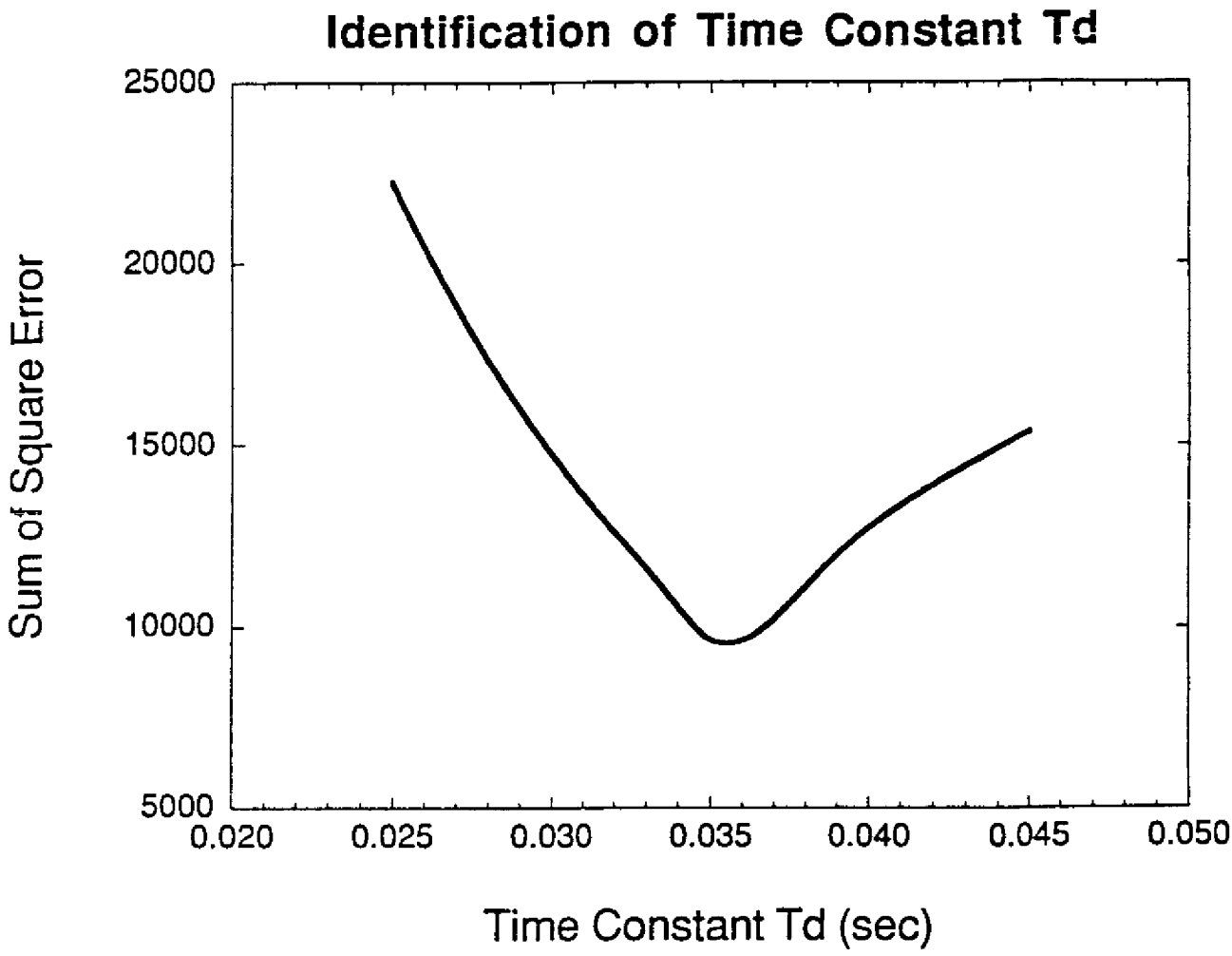

Figure 4.3: Identification of Time Constant T_d

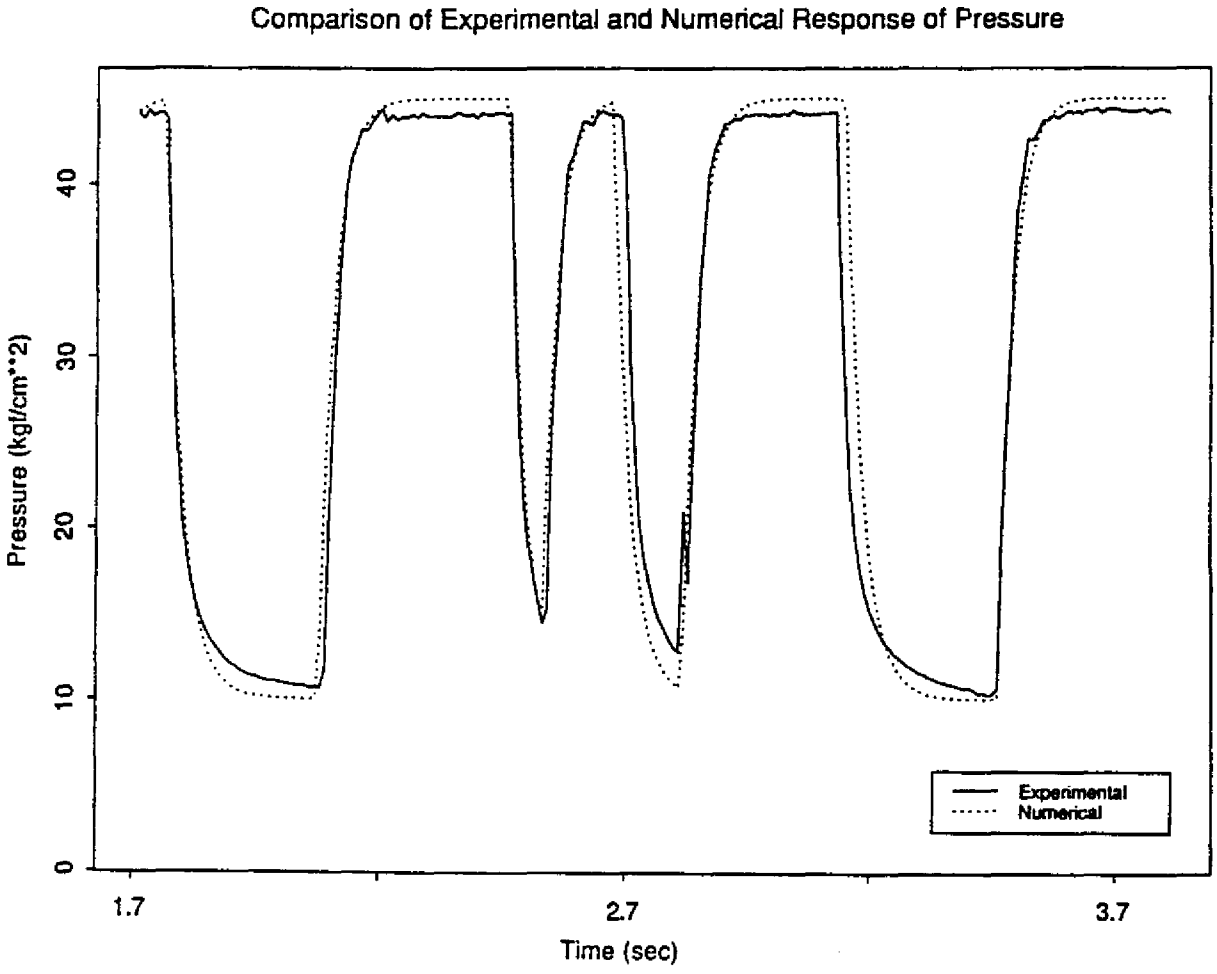

Figure 4.4: Example of Experimental and Simulated Time Histories of Pressure

of 10 kgf/cm^2 can, for example, be reduced to 1.6% at the pressure of 45 kgf/cm^2. Equation 2.7 thus can be used to describe the relationship, and the values of c_1 and c_2 are identified as $c_1 = 2.4\text{cm}^3/\text{s}^2\text{kgf}$ and $c_2 = 124.0\text{cm/s}$. As will be shown in the next subsection, however, the friction force depends not only on the pressure but also on the sliding velocity. In this respect, the value of normalized friction force used in Eq. 2.7 is valid only when the sliding velocity is zero, and therefore it is rewitten as

$$f_0 = -c_1 p + c_2 \tag{4.1}$$

where f_0 is the normalized friction force at sliding velocity of zero.

4.1.3 Dependence of Friction on Sliding Velocity

It is observed from the response acceleration measured in Experimental Series 1 (passive isolation) that the the normalized friction force f decreases with the increase of sliding velocity. In fact, these measurements are used to identify the dependence of friction on sliding velocity.

Figure 4.6 shows an example set of time histories of a passive isolation experiment, in which the pressure was kept at 30 kgf/cm^2, corresponding to the coefficient of friction 5.6%, and the input ground motion was El Centro record with peak acceleration of about 300 gal. From the behavior of the response acceleration, it is assumed that the relationship between the normalized friction force and sliding velocity takes the following analytical form:

$$f = f_0 \frac{k^2}{\dot{x}^2 + k^2} \tag{4.2}$$

where f_0 is the normalized friction at sliding velocity of zero as defined by Eq. 3.2, while k is a constant.

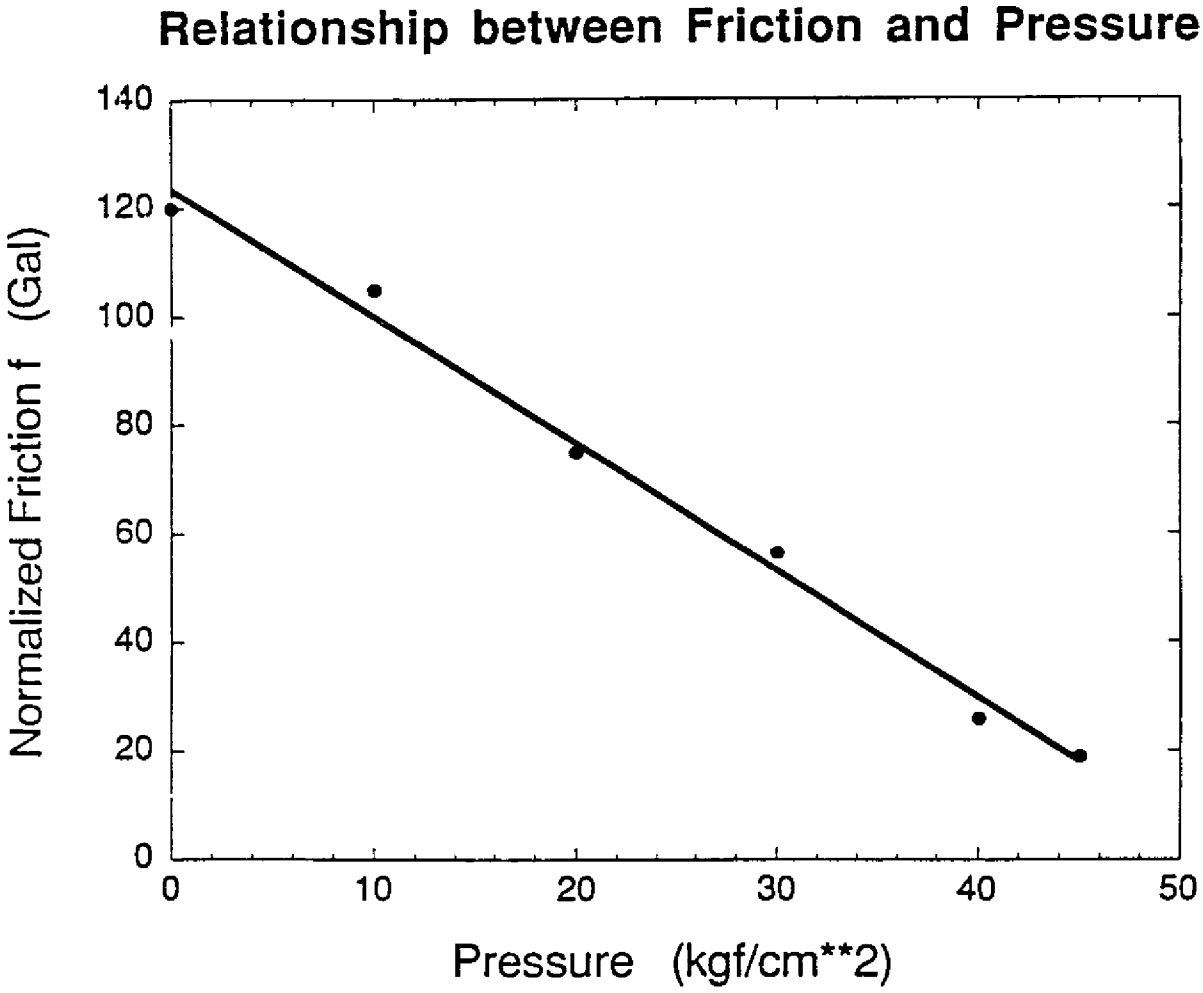

Figure 4.5: Relationship between Pressure and Normalized Friction Force

Table 4.1: Identified Parameters

T_i	29 ms	c_1	2.4 $cm^3/(s^2kgf)$
T_d	35 ms	c_2	124.1 cm/s^2
k^2	0.11 cm/s		

The value of k^2 is identified by minimizing the sum of the square errors between response acceleration shown in Fig. 4.7 and that from the numerical simulation over the entire time history $(\sum_k ((\ddot{x}+\ddot{z})_{sim}(t_k;k) - (\ddot{x}+\ddot{z})_{exp}(t_k))^2)$. As shown in Fig. 4.7, the optimal value of k^2 is 0.11 m^2/s^2, at which the sum of square error is minimum.

It is found that $k^2 = 0.11$ m^2/s^2 is also the optimal value for other passive isolation experiments where the pressure is kept at 10, 20, 40 and 45 kgf/cm^2. Figure 4.8 shows part of the experimental and simulated time histories of response acceleration for the passive isolation performed under $p = 30$ kgf/cm^2. Again, the simulation result matches the experimental result very well, implying that the identified model for friction closely represents the reality.

4.1.4 Response of Friction to Control Signal

Summarizing the identification results, the response of friction force to control signal can be modeled by the following equations:

$$T\dot{p} + p = u \tag{4.3}$$

$$f_0 = -c_1 p + c_2 \tag{4.4}$$

$$f = f_0 \frac{\dot{x}^2}{\dot{x}^2 + k^2} \tag{4.5}$$

The values of parameters T, c_1, c_2, k^2 identified are summerized in Table 4.1.

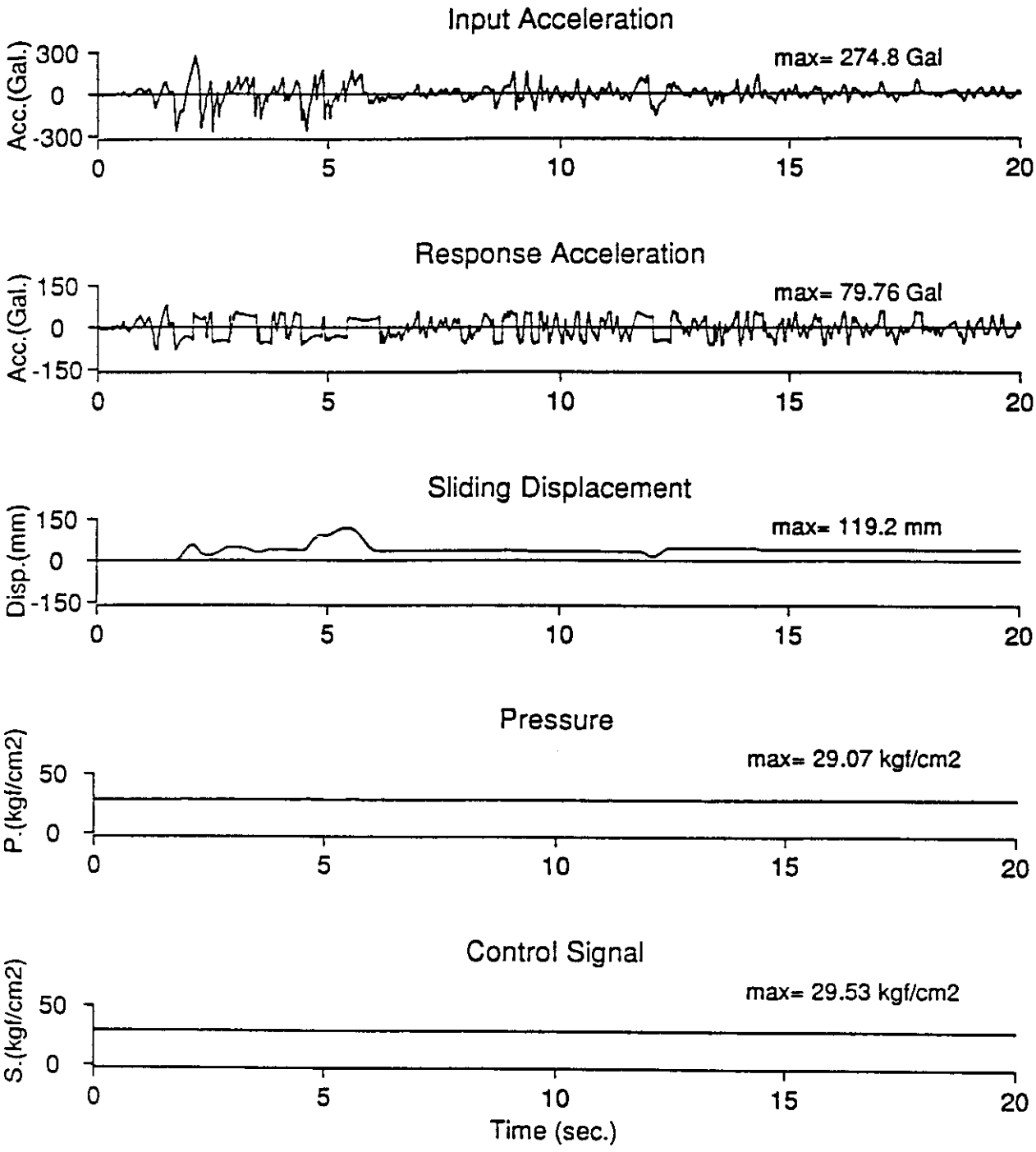

Figure 4.6: Passive (Experiment)

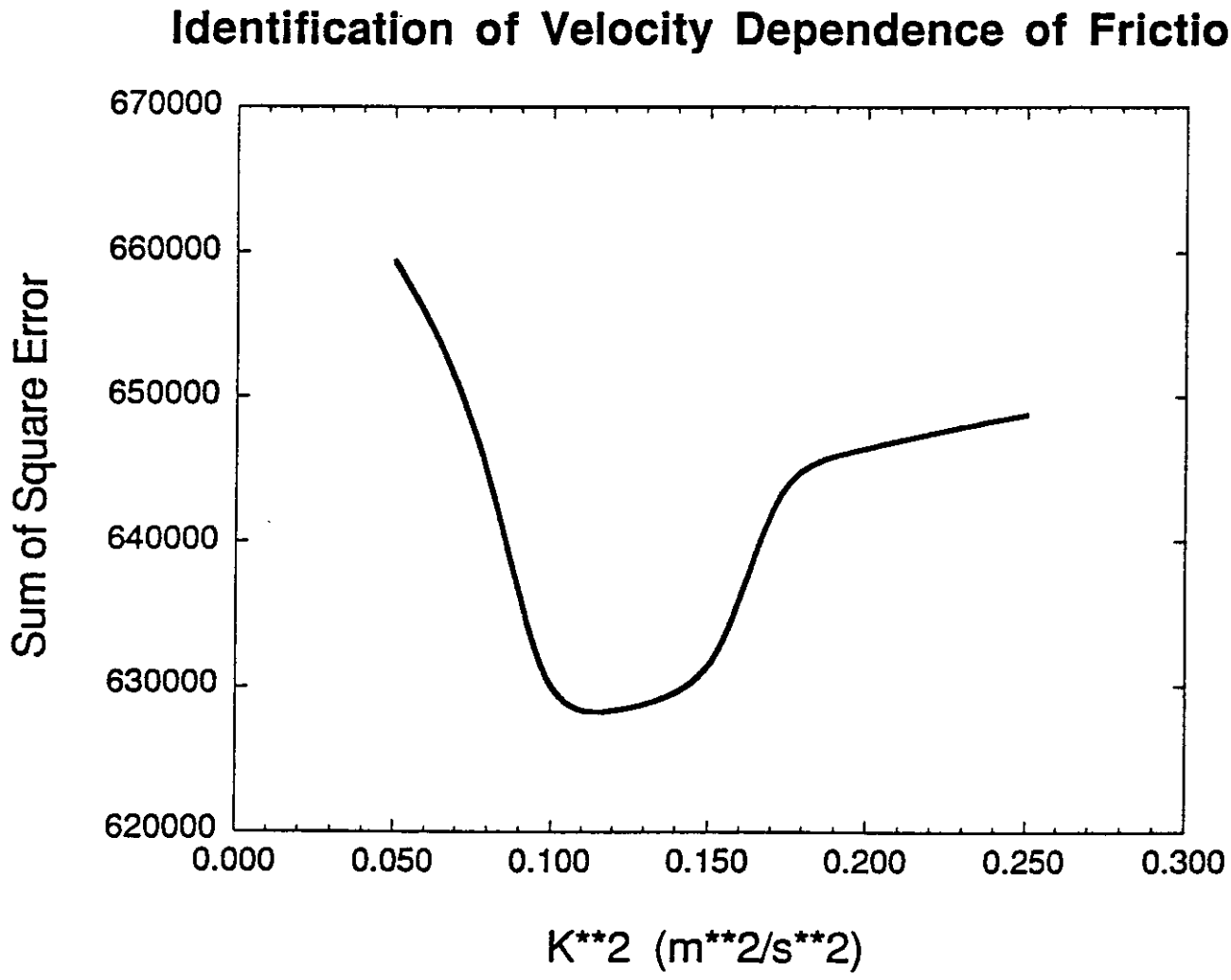

Figure 4.7: Identification of Constant k^2

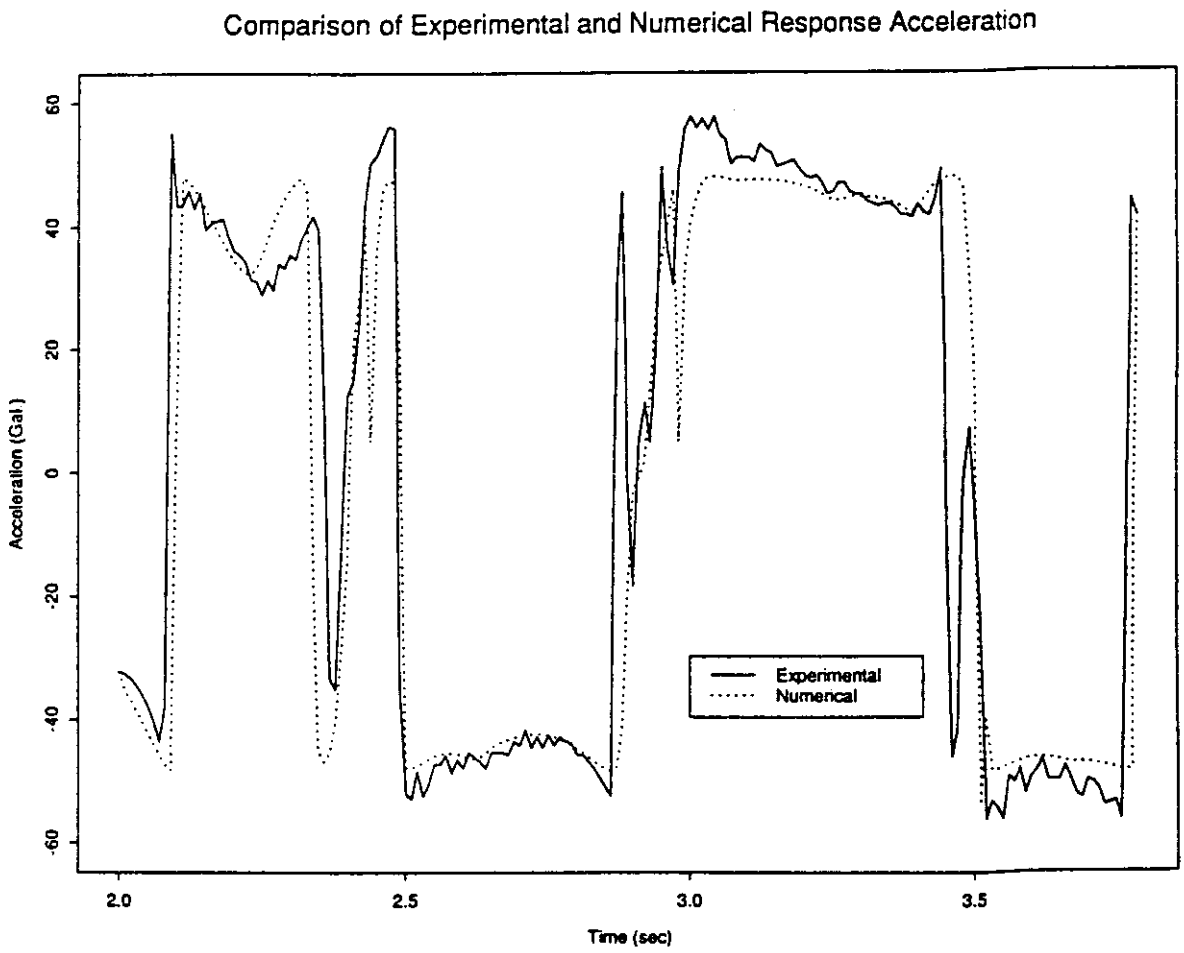

Figure 4.8: Example of Experimental and Simulated Time Histories of Acceleration

4.2 Passive and Hybrid Isolation

Typical experimental results from four series of experiments utilizing the techniques of passive isolation, bang-bang control, and instantaneous optimal control with and without time delay are compared with each other. These results are obtained under the El Centro (NS, 1940) ground motion with the peak acceleration of about 300 Gal. Figures 4.6 and 4.1 shown before give two sets of time histories for response acceleration, sliding displacement, pressure, and pressure control signal corresponding to Experimental Series 1 and 2 respectively, while Figs. 4.9 and 4.10 show two sets corresponding to Experimental Series 3 and 4.

In the passive isolation results as shown in Fig. 4.6, the pressure in the bearing chamber was kept at 30 kgf/cm^2, corresponding to the coefficient of friction 5.6%. A large residual sliding displacement of 62 mm after the earthquake is observed.

In the bang-bang control experiment shown in Fig. 4.1, the pressure control signal is switched between 10 kgf/cm^2 and 45 kgf/cm^2. The maximum and minimum response accelerations are consistent with the accelerations of the passive isolation cases of p = 10 kgf/cm^2 and 45 kgf/cm^2 respectively. However, the residual displacement is almost zero and the maximum sliding displacement is about 20 % less than the passive isolation, showing the effectiveness of the bang-bang control in reducing the sliding displacement.

Figures 4.9 and 4.10 respectively show the results of hybrid isolation experiments using instantaneous optimal control without and with time delay, in which the feedback gains are set to: F_f = 1.0 kgfs^2/cm^3 and F_d = -45 kgf/cm^3, and F_f = 16.5 kgf/cm^2 and F_d = -16.4 kgf/cm^3 with time delay. In both cases, the pressure control signal is confined between u_{max} = 45 kgf/cm^2 and u_{min} = 10 kgf/cm^2. The response of instantaneous optimal control,

depicted in Figs. 4.9 and 4.10, show the results similar to that of the bang-bang control experiment. This is because the feedback gains used in these experiments force the control signal to reach the minimum value of 10kgf/cm^2 primarily for the purpose of confining the sliding displacement to a small value under the ground acceleration as large as El Centro earthquake with peak acceleration of about 300 gal. The instantaneous optimal control with time delay (Fig. 15(a)) shows the best control performance among the three control algorithms developed and tested in the experiments.

The difficulty of starting initial slide associated with the passive system is alleviated in the hybrid systems.

The experimental results of passive and hybrid isolation under the Hachinohe (NS) and Taft (EW) are shown in the Appendex A.

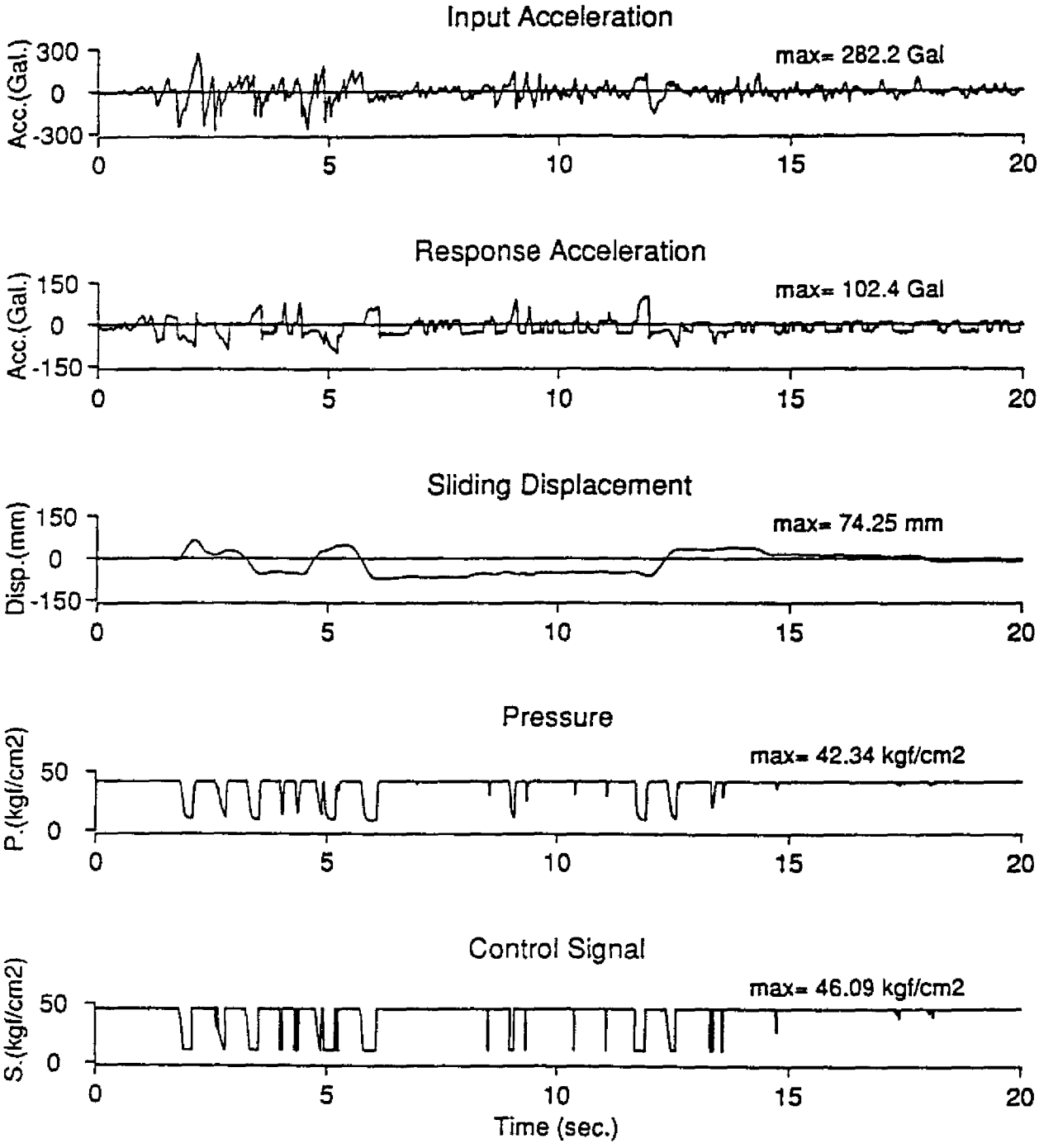

Figure 4.9: Instantaneous Optimal Control without Time Delay (Experiment)

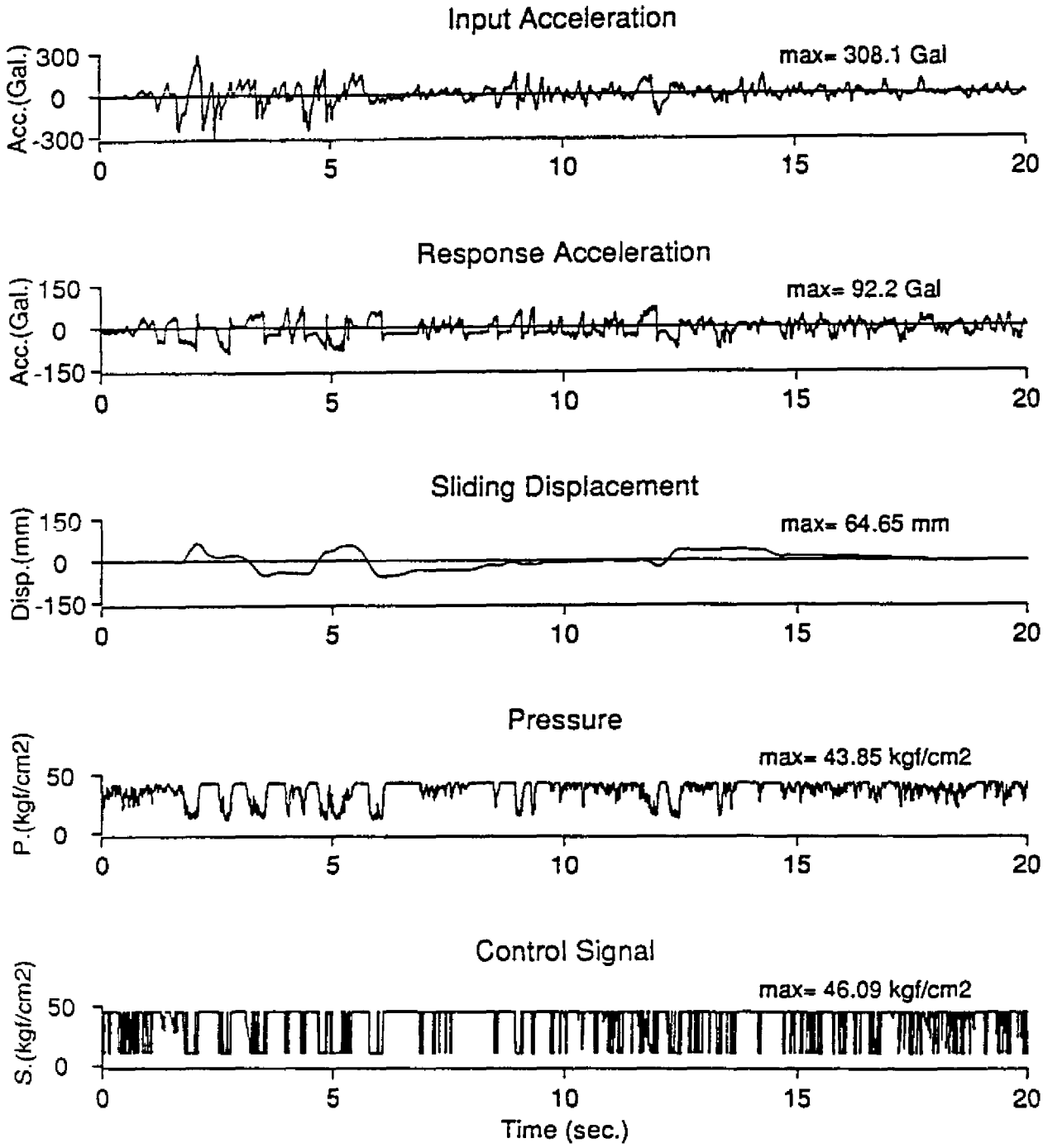

Figure 4.10: Instantaneous Optimal Control with Time Delay (Experiment)

4.3 Comparison of Hybrid and Passive Isolation

The performance of the hybrid isolation system is compared to that of the passive isolation system. Figures. 4.11 and 4.12 show the maximum response acceleration, maximum sliding displacement, and the residual displacement of the structural model with passive or hybrid isolation system under El Centro records of different peak ground acceleration. Hybrid isolation results shown in these figures are those under instantaneous optimal control algorithm without time delay.

In the passive isolation, if a small friction coefficient, for example 1.6%, is used, a high level of isolation performance is expected since the response acceleration is reduced to a small level. In this case, however, the maximum displacement becomes excessive very rapidly as the input earthquake becomes more intense. On the other hand, if a large friction coefficient such as 10.2% is used, the sliding displacement can be confined within a relatively small range. However, the isolation performance in this case is limited in the sense that the acceleration can not be satisfactorily reduced. Particularly for small to medium earthquakes with peak acceleration less than 100 gal, this passive sliding isolation system does not function at all, thus the response acceleration equals the input acceleration. Such acceleration might damage the sensitive equipment inside the building.

The hybrid isolation system, however, can alleviate these problems associated with the passive isolation system. For small to medium earthquakes, the friction can be controlled to a very small level to make the structure slide easily, so that the response acceleration can be considerably reduced. For large earthquakes, the friction is controlled to prevent the excessive sliding displacement, while the response acceleration can also be kept at a small level. Another advantage of the hybrid system is clearly seen in Fig. 4.12 where the residual

sliding displacement can be maintained almost at zero level.

Experimental results verify that the proposed friction controllable sliding system does make the conventional passive sliding isolation system effective for all intensities of earthquake.

Comparison of Response Acceleration

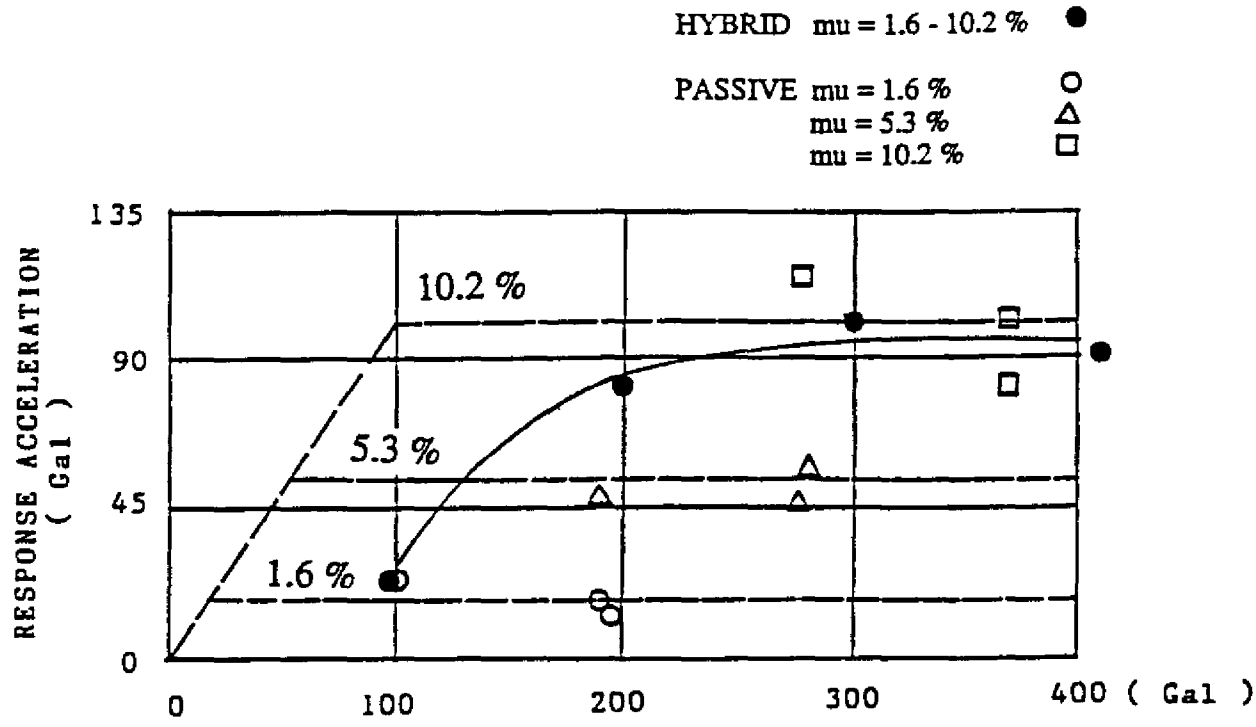

Comparison of Sliding Displacement

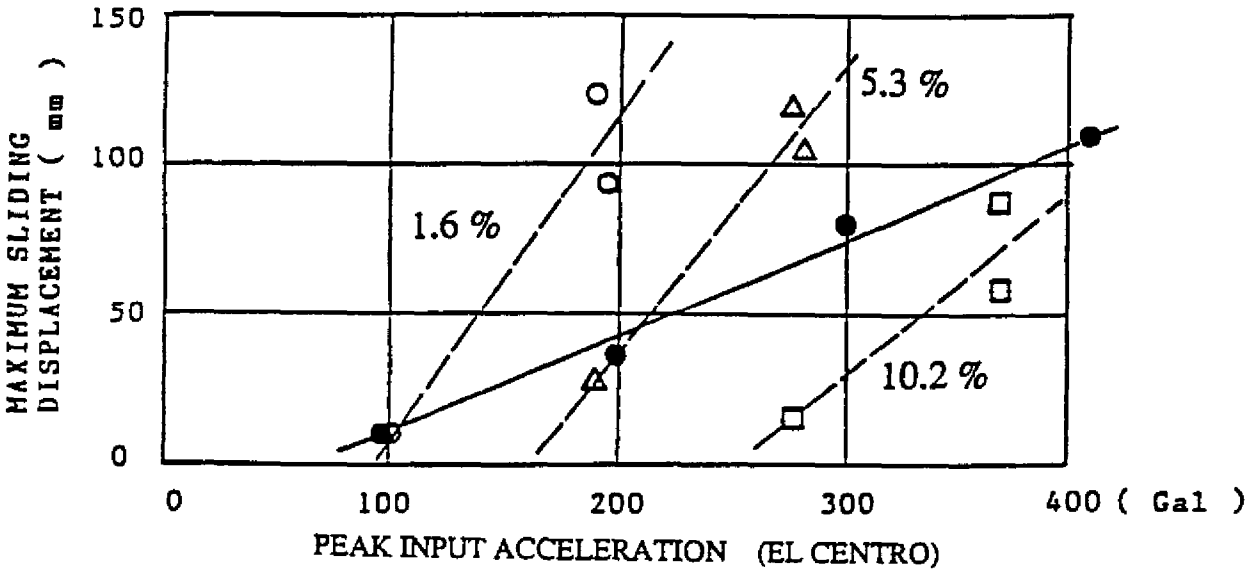

Figure 4.11: Comparison of Passive and Hybrid Isolation

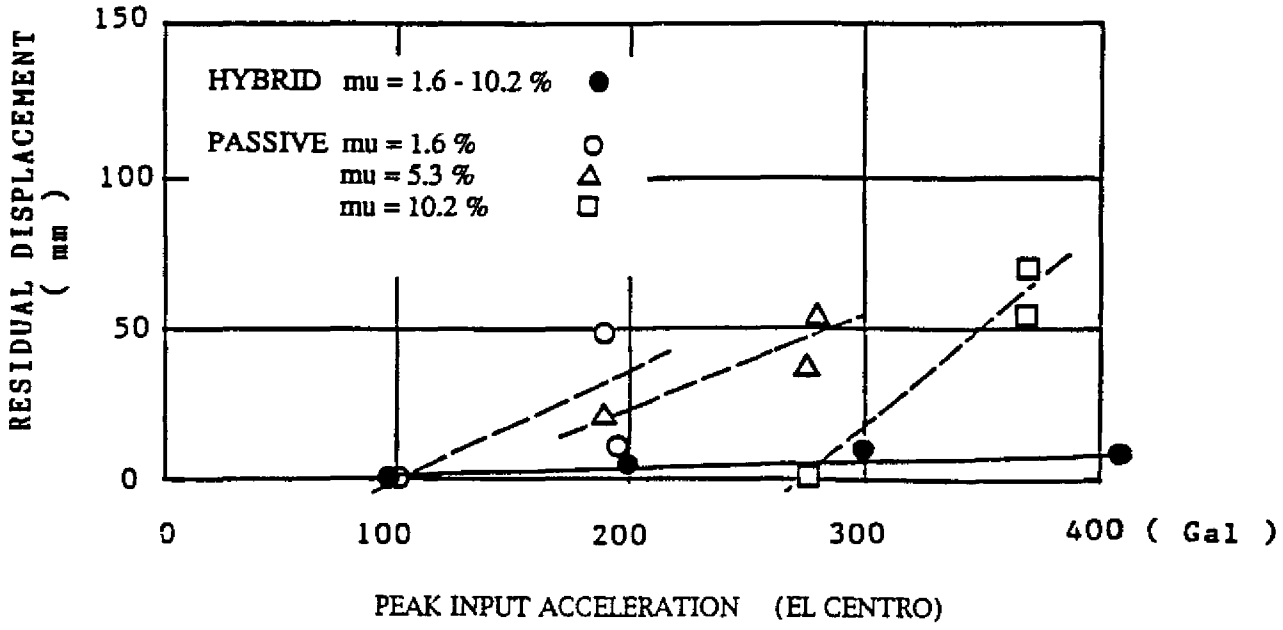

Figure 4.12: Comparison of Passive and Hybrid Isolation (Residual Displacement)

4.4 Study of Control Parameters

The effects of control parameters, such as the time interval of control Δt_c and the threshold value for the window comparator, on control performance have been studied in shaking table experiments. On the basis of these studies, the appropriate values of these parameters are determined. Although the values of feedback gains were also examined in a few cases of shaking table experiments, they were determined by computer simulation analysis.

4.4.1 Time Interval of Control

The continuous-time control algorithms developed in Section 2 can only be executed in the discrete time since a digital computer is used for on-line computation and control execution. As a consequence, response measurements are digitized as feedback signals, while control signal is sent in the form of piecewise step functions through the analog-digital converter as shown in Fig. 3.6. Hence, they are not continuous functions as called for by continuous-time control algorithms, and usually the larger the time interval for control execution, the worse the control performance becomes.

For this reason, the effect of the time interval of control on control performance has been studied in shaking table experiments performed for hybrid isolation system. The response time histories obtained in the experimental case identified as 6-3 with the time interval of control $\Delta t_c = 0.030$ sec, and experimental case identified as 6-6 with $\Delta t_c = 0.004$ sec, are shown respectively in Figs. 4.13 and 4.14. Both cases are under instantaneous optimal control without consideration of time delay, and are subjected to El Centro 300 Gal input earthquake. The time interval for the measurement of feedback signals are $\Delta t_d = 0.002$ sec in both cases.

In the response acceleration shown in Fig. 4.13 (Case 6-3), impulsive response behaviors are observed (denoted by ∇). They are, however, mostly eliminated in Case 6-6 as shown in the same figure indicating the improvement of control performance by reducing the time interval of control. The sliding displacements, however, show little difference between these two cases as seen in Fig. 4.14.

Further inverstigation shows that the time interval of control smaller than 0.004 sec does not significantly improve control performance. Hence, the time interval of control Δt_c has been set at 0.004 sec in all other control experiments.

It is also interesting to find that the time interval does not change the basic behavior of the structual response without introducing instability. For example, even the time interval as large as 0.03 sec does not introduce the instability of the control system as shown in Figs. 4.13 and 4.14. In this sense, this hybrid control system is quite robust.

4.4.2 Window Comparator

From the control experiments, it was found that there was some high frequency noise in the measurement of feedback signals which resulted in undesirable control signal. In fact, the use of the feedback signal including such high frequency components in experiments produced highly inefficient control results. To alleviate this difficulty, a practical method called "window comparator" is used. The method simply defines a certain threshold value, for the increment of a feedback signal over a certain time interval. If the increment is below the threshold, the variation in the feedback signal is considered as noise and the feedback signal is considered unchanged over that time interval.

The appropriate threshold values for displacement and acceleration signals were studied

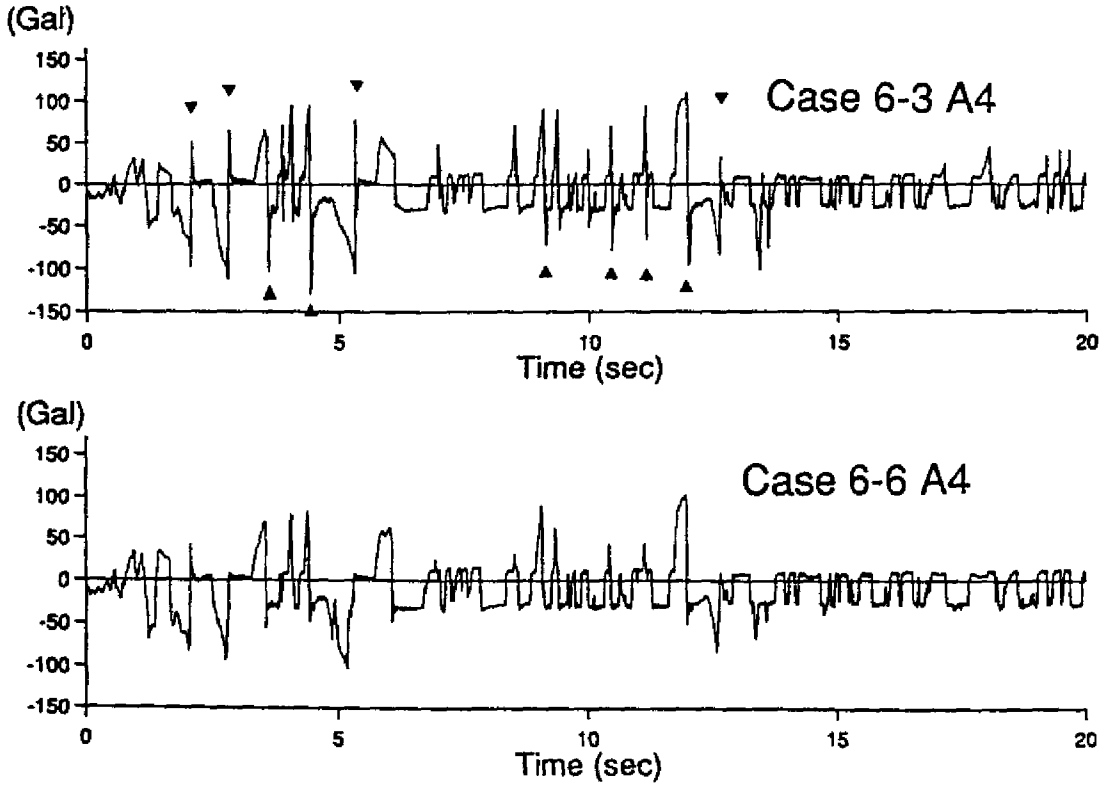

Figure 4.13: Effect of Control Time Interval on Response Acceleration

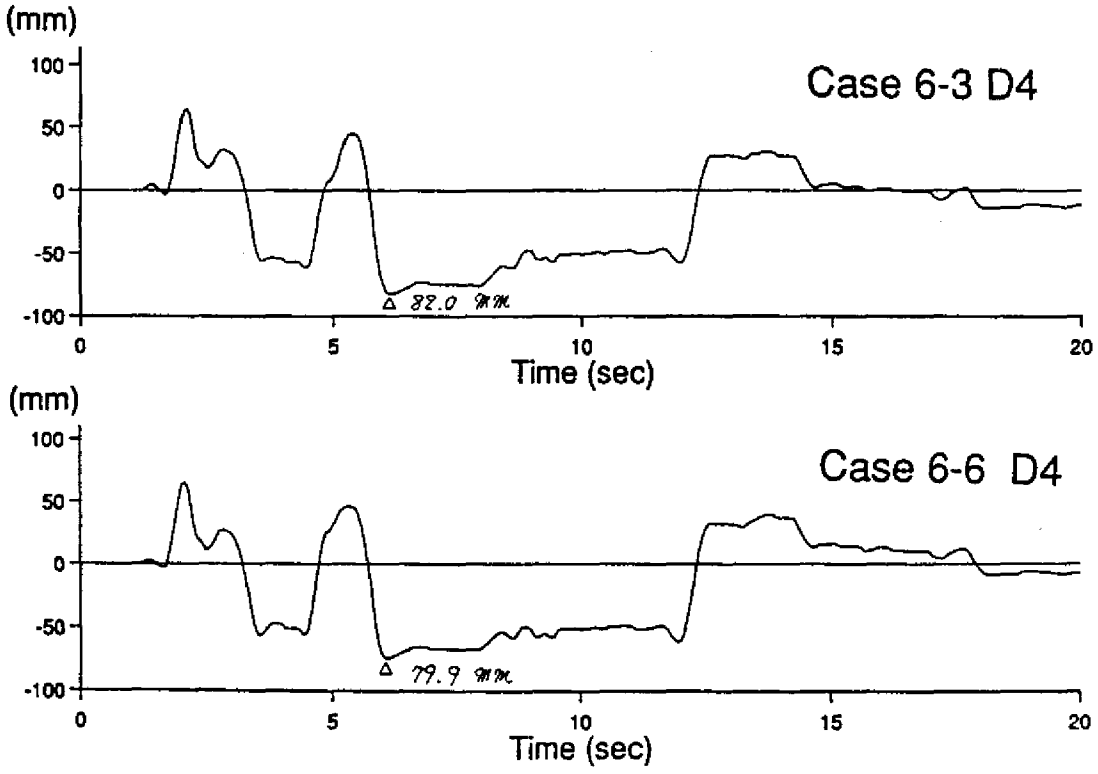

Figure 4.14: Effect of Control Time Interval on Sliding Displacement

respectively in hybrid isolation experiments using instantaneous optimal control with and without time delay. As a result, the threshold value for displacement signal was determined to be $\Delta x = 0.02$ cm for every two control time intervals of 0.008 sec, and the threshold value for acceleration signal was determined to be $\Delta(\ddot{x} + \ddot{z}) = 0.75$ gal for each control time interval of 0.004 sec. The control results are dramatically improved when these threshold values are used. To examine the significance of the threshold values, the increment Δx measured in displacement x measured for every time interval of 0.008 sec from an optimal control experiment is plotted at the end of each time interval as shown in Fig. 4.15, together with time history of displacement. This figure shows that the threshold value equal to 0.02 cm for the displacement increment consistently removes the noise-like high frequency components of the feedback signal.

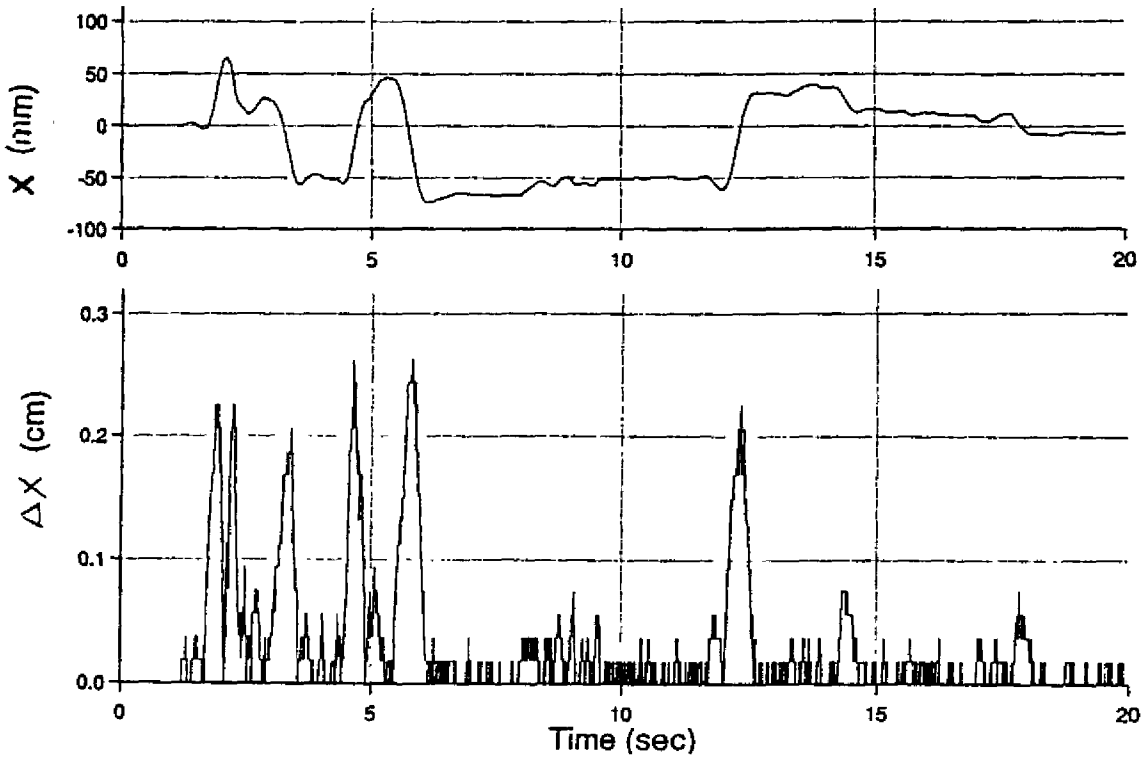

Figure 4.15: Study of Window Comparator